Propagation of Photosensitive Chemical Waves on the Circular Routes

Hiroyuki Kitahata,[†] Akiko Yamada,[‡] Satoshi Nakata,*[,‡] and Takatoshi Ichino[†,§]

Department of Physics, Graduate School of Science, Kyoto University, Kyoto 606-8502, Japan, and Department of Chemistry, Nara University of Education, Takabatake-cho, Nara 630-8528, Japan

Received: February 15, 2005; In Final Form: April 6, 2005

The propagation of chemical waves in the photosensitive Belousov−Zhabotinsky (BZ) reaction was investigated using an excitable field in the shape of a circular ring or figure "8" that was drawn by computer software and then projected on a film soaked with BZ solution using a liquid-crystal projector. For a chemical wave in a circular reaction field, the shape of the chemical wave was investigated depending on the ratio of the inner and outer radii. When two chemical waves were generated on a field shaped like a figure "8" (one chemical wave in each circle) as the initial condition, the location of the collision of the waves either was constant or alternated depending on the degree of overlap of the two circular rings. These experimental results were analyzed on the basis of a geometrical discussion and theoretically reproduced on the basis of a reaction−diffusion system using a modified Oregonator model. These results suggest that the photosensitive BZ reaction may be useful for creating spatio-temporal patterns depending on the geometric arrangement of excitable fields.

Introduction

Experimental and theoretical studies on wave propagation on an excitable media may help us not only to understand signal processing in biological systems[1] such as nerve impulses[2,3] but also to create novel methods for artificial processing such as image processing[4−7] and logic operations.[8−13] The Belousov−Zhabotinsky (BZ) reaction has been widely investigated as an excitable and oscillatory chemical system.[14−16] The BZ reaction on a membrane, e.g., filter paper,[17,18] Nafion membrane,[19−21] gel,[22,23] or glass filter,[24] has been well studied because the spatio-temporal pattern of wave propagation can be regulated by the geometry of the excitable field, which is prepared by cutting[17] or printing.[18] In such systems, however, it can be technically difficult to cut a membrane filter with a complex geometry and to regulate the number of chemical waves and their intervals.

A photosensitive experimental setup of the BZ reaction[4,25] makes it easy to create excitable fields of various geometries, which are drawn by computer software and then projected on a film soaked with BZ solution using a liquid-crystal projector.[13,26] In this case, light illumination produces bromine, which inhibits the oscillatory reaction; i.e., the degree of excitability can be adjusted by changing the intensity of illumination. Therefore, the number of chemical waves and their intervals can be spatio-temporally regulated by illumination.[13,27]

In this study, the propagation of chemical waves in the photosensitive BZ reaction on an excitable field (a circular ring or a figure "8" composed of two equivalent circular rings) illuminated with a liquid-crystal projector was investigated. The nature of wave propagation depending on the ratio of the inner and outer radii of the circular rings was well fitted as the involute of a circle.[28−31] When the two equivalent circular rings slightly in contact one another, two chemical waves collided at a location apart from the intersection. When the circular rings of the figure "8" completely overlapped, the location of wave collision alternated with time. The essential feature of wave propagation was qualitatively reproduced by a computer simulation based on the reaction−diffusion equation using a modified Oregonator model.

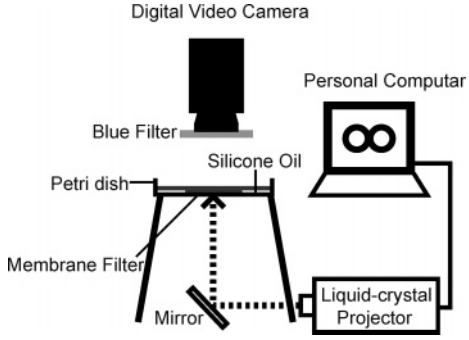

Figure 1. Schematic illustration of the experimental system based on the photosensitive BZ reaction.

Experiments

$Ru(bpy)_3Cl_2$, which was purchased from Sigma-Aldrich (St. Louis, MO), was used as a catalyst for the photosensitive BZ reaction. The BZ solution consisted of $[NaBrO_3] = 0.45$ M, $[H_2SO_4] = 0.3$ M, $[CH_2(COOH)_2] = 0.2$ M, $[KBr] = 0.05$ M, and $[Ru(bpy)_3Cl_2] = 1.7$ mM. Cellulose−nitrate membrane filters (Advantec, A100A025A) with a pore size of 1 μm were soaked in BZ solution (5 mL) for about 1 min. The soaked membrane was gently wiped with filter paper to remove excess solution and placed on a Petri dish (diameter: 100 mm). The surface of the membrane filter was completely covered with 1 mL of silicone oil (Wako, WF-30) to prevent it from drying and to protect it from the influence of oxygen. The experiments were carried out in an air-conditioned room at 298 K, at which

* To whom correspondence should be addressed. Tel.& fax: +81-742-27-9191. E-mail: nakatas@nara-edu.ac.jp.
† Kyoto University.
‡ Nara University of Education.
§ Present address: Department of Intelligent Systems, Kinki University, Wakayama 649-6493, Japan.

10.1021/jp0507905 CCC: $30.25
Published on Web 05/14/2005

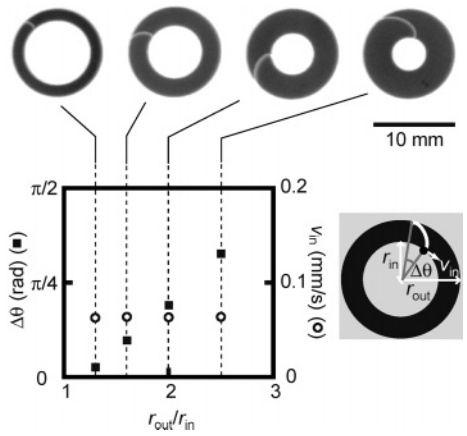

Figure 2. Wave propagation in a circular ring depending on r_{out}/r_{in} for v_{in} (empty circle) and $\Delta\theta$ (filled square). Corresponding snapshots are indicated (top view) above the figure. $\Delta\theta$, r_{out}, r_{in}, and v_{in} are schematically defined at the right side of the figure.

the reaction medium showed no spontaneous excitation and no change in behavior for approximately 30 min.

The medium was illuminated from below, as schematically shown in Figure 1. The high-pressure mercury bulb of a liquid-crystal projector (MITSUBISHI, LVP-XL8) was used as a light source and the spatial intensity distribution was controlled by a personal computer. A black and white picture on the liquid-crystal projector served as an illumination mask to create the appropriate boundary, and the light intensities were 4.0×10^2 lx for black and 1.7×10^4 lx for white. The experiments were monitored from above with a digital video camera (SONY, DCR-VX700) and recorded on videotape. A blue optical filter (Asahi Techno Glass, V-42) with a maximum transparency at 410 nm was used to enhance the image of the chemical waves. The light intensity at the illuminated part was measured with a light intensity meter (AS ONE, LX-100).

Results

a. Propagation of a Single Wave on a Circular Ring. First, we examined the radius-dependent propagation of a single wave on a reaction field in the shape of a circular ring. In this experiment, two chemical waves initially propagated in opposite directions. By locally increasing the illumination around one wave within 1 s, the illuminated wave was disappeared, but another one continued to propagate. Therefore, the unidirectional chemical wave on the ring could be achieved. Figure 2 shows the velocity of wave propagation on a circular ring depending on r_{out}/r_{in} (r_{in} = inner radius, r_{out} = outer radius of the circular route). In this experiment, r_{in} was varied under constant r_{out} (=6 mm). The velocity of the chemical wave at the inner boundary of the circle (v_{in}) was almost independent of r_{in}. On the other hand, that at the outer boundary (v_{out}) was linearly increased with $1/r_{in}$, which indicates that the angular velocity of the chemical wave (ω) was determined by the wave propagation near the inner radius, i.e., $\omega = (v_{in}/2\pi)/r_{in}$ and $v_{out} = 2\pi r_{out}\omega$. The phase difference ($\Delta\theta$), which is schematically defined in Figure 2, increased with r_{out}/r_{in}; i.e., the deformation of the chemical wave increased with the width of the circular ring.

b. Collision of Two Chemical Waves on Two Equivalent Circular Rings. Next, we examined the interaction between

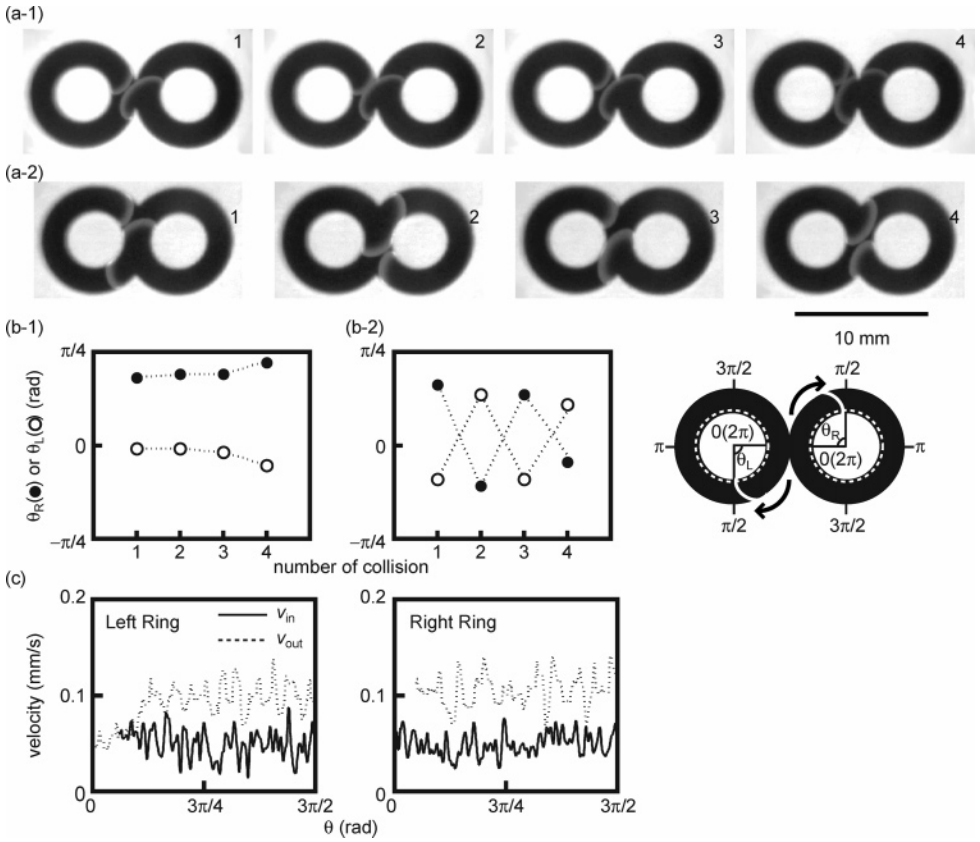

Figure 3. Interactive wave propagation between two chemical waves in two equivalent circular rings that (1) were slightly in contact and (2) completely overlapped one another. (a) Top view of the snapshots of the wave propagation with the time intervals of (1) 300 s and (2) 250 s. (b) θ_R (filled circle) and θ_L (empty circle) when the two waves collided for (b-1) slightly connecting rings and (b-2) completely overlapping rings. θ_L and θ_R were the polar coordinates on the inside of the rings and were schematically defined on the right side. The numbers of collision (1−4) correspond to those in (a). (c) v_{in} (solid line) and v_{out} (dotted line) versus θ for the left and right rings in (1).

two chemical waves on a reaction field composed of two equivalent circular rings at $r_{in} = 2.1$ mm and $r_{out}/r_{in} = 2.0$. In this experiment, one chemical wave was initially generated in each ring in the same direction (clockwise), and the chemical wave in the right ring reached the intersection before that in the left ring.

When the distance between the centers of the two rings was nearly equal to $2r_{out}$, i.e., the two rings were just slightly in contact with one another, the location of the collision of the two waves was determined to be in the left ring near the intersection, as shown in Figures 3a-1 and b-1. Here, θ_L and θ_R are the angles corresponding to the positions of chemical waves on the left and right inner rings, and they are plotted at the moment two pulses collide in Figure 3b. The location of the collision converged from 1.82π rad at the initial collision to 1.93π rad with time, and this convergent value did not change even when the difference in the initial phases was smaller than 1.93π rad (data not shown).

v_{in} and v_{out} for two rings were measured to clarify why the location of collision was apart from the intersection. For the left ring, v_{in} was almost equal to that in the right ring (0.05 mm/s) except for around the intersection (see "Left Ring" in Figure 3c). v_{out} was nearly equal to v_{in} when the chemical wave propagated without contacting the inner boundary at $\theta = 0$ to $\pi/6$ rad. When the chemical wave was in contact with the inner boundary, v_{out} was accelerated and then reached a constant value (0.10 mm/s) at around $\theta = \pi/2$ rad (see "Left Ring" in Figure 3c). For the right ring, v_{in} and v_{out} were almost constant except for around the intersection (see "Right Ring" in Figure 3c).

When the distance between the centers of the two rings was equal to $r_{in} + r_{out}$, i.e., the two rings completely overlapped one another, the location of the collision of the two waves changed alternatively, as shown in Figures 3a-2 and b-2. The location of the collision location changed alternatively to either the right ring or the left ring; i.e., the chemical wave from the right ring reached the intersection ahead of that from the left ring, as seen in snapshots **1** and **3**, or vice versa, as seen in snapshots **2** and **4**.

Discussion

a. Nature of Chemical Wave Propagation in a Single Circular Ring. On the basis of the experimental results and those in a related paper,[28−31] we now discuss the characteristics of the BZ wave propagation in a reaction field that is geometrically illuminated. First, we analyze the shape of wave propagation depending on r_{out}/r_{in} of the circular ring. If we suppose that the wave propagates on the reaction field without any effects from the boundary, and that the wave cannot move into the brighter area, the distance from a point on the inner circle (point α) to another point (point β), which is one of the locations at which the chemical wave propagates along the inner circle, is the same as that to the intersection (point γ) between the chemical wave and the tangent line at the noted point (point α), as schematically indicated in Figure 4a, because the chemical wave propagates in a direction perpendicular to the chemical wave with a uniform velocity. Therefore, the shape of the chemical wave may be regarded as the involute of a circle.[28−31]

From a geometrical perspective, when the location of the chemical wave on the inner circle of the ring (point β) is expressed as $x = r_{in} \cos \theta_{in}$ and $y = r_{in} \sin \theta_{in}$, that on the chemical wave is expressed using parameter θ,

$$\begin{pmatrix} x \\ y \end{pmatrix} = r_{in}\begin{pmatrix} \cos\theta \\ \sin\theta \end{pmatrix} + r_{in}(\theta_{in} - \theta)\begin{pmatrix} -\sin\theta \\ \cos\theta \end{pmatrix} \quad (1)$$

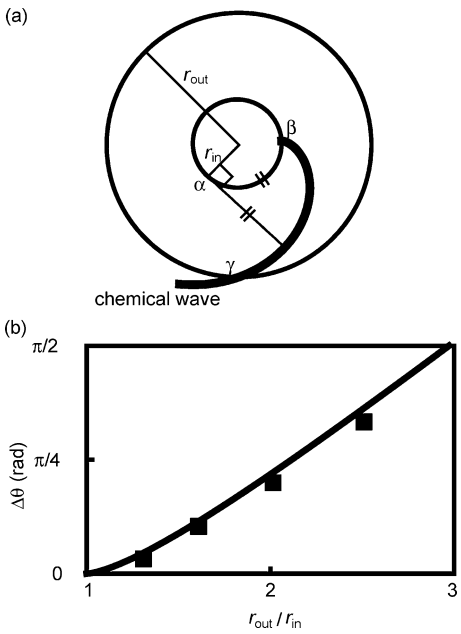

Figure 4. Comparison of the experimental results and the analytical prediction. (a) Schematic representation on the shape of the "involute" of a circle. (b) (Solid squares) experimental results and (solid curve) analytical prediction based on eq 6.

We calculate the location of the intersection between the chemical wave and the outer circle with a radius of r_{out} (point γ). Here, the phase of the intersection is set as θ_{out}. From

$$r_{out}^2 = r_{in}^2(1 + (\theta_{in} - \theta)^2) \quad (2)$$

and

$$\tan\theta_{out} = \frac{r_{in}\sin\theta + r_{in}(\theta_{in} - \theta)\cos\theta}{r_{in}\cos\theta - r_{in}(\theta_{in} - \theta)\sin\theta} = \frac{\tan\theta + (\theta_{in} - \theta)}{1 - (\theta_{in} - \theta)\tan\theta} \quad (3)$$

we can get

$$\tan\theta_{out} = \tan(\theta_{in} + \alpha) \quad (4)$$

where $\tan\alpha = \sqrt{r_{out}^2 - r_{in}^2}/r_{in} = \theta_{in} - \theta$. From eq 4,

$$\theta_{out} = \theta_{in} + \alpha = \theta_{in} - \sqrt{r_{out}^2 - r_{in}^2}/r_{in} + \arctan(\sqrt{r_{out}^2 - r_{in}^2}/r_{in}) \quad (5)$$

Therefore, we can derive

$$\Delta\theta = \theta_{in} - \theta_{out} = \sqrt{(r_{out}/r_{in})^2 - 1} - \arctan(\sqrt{(r_{out}/r_{in})^2 - 1}) \quad (6)$$

Figure 4b shows the theoretical results obtained on the basis of eq 6. These theoretical results suggest that the experimental results regarding the nature of the chemical wave propagation shown in Figure 4 can be quantitatively fitted by a theoretical consideration based on the geometrical discussion. In a previous study, several researchers reported that the shape of the chemical wave is the involute of a circle and that it can be regarded as an Archimedes spiral far enough from the tip of the wave.[28−31] In this study, the chemical wave is well fit to the involute of a circle but not a spiral, because the core of the spiral is much larger than that of the spiral pattern formed spontaneously.

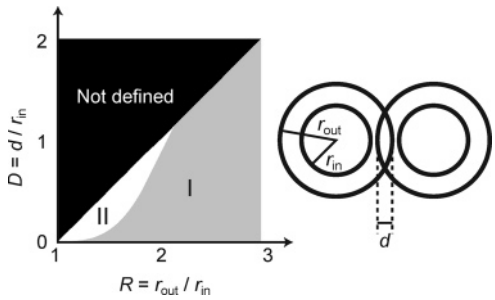

Figure 5. Phase map of the synchronization of chemical wave propagation in a reaction field composed of two equivalent circular rings depending on $R = r_{out}/r_{in}$ and $D = d/r_{in}$. Region I corresponds to collision at one point, and region II corresponds to alternative collisions.

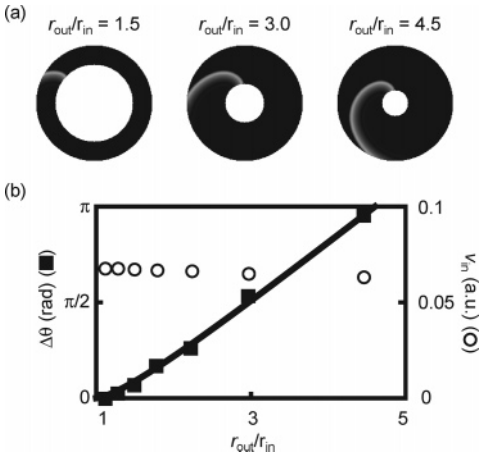

Figure 6. Results of the numerical simulation for a reaction field in the shape of a circular ring based on the modified Oregonator model shown in eqs 7 and 8. (a) Snapshots for the various values of r_{out}/r_{in}. (b) Wave velocity along the inner boundary v_{in} (empty circle) and the phase difference between the locations of the chemical wave along the inner and outer boundaries $\Delta\theta$ (filled square) depending on r_{out}/r_{in}. The curve derived from the analytical discussion is also described as a solid curve.

b. Nature of Chemical Wave Propagation on Two Equivalent Circular Rings. Following the above discussion, we calculated the nature of chemical wave propagation in a reaction field composed of two equivalent circular rings. We derived a characteristic phase difference $\Delta\theta_0$ that depended on the shape of the reaction field. First, it should be noted that there are two types of interaction between the chemical waves on the two rings: in one type, the chemical wave on one ring (ring A) propagates and touches the inner radius of the other ring (ring B), and in the other type, the chemical wave does not touch it. In the former case, the phase of the chemical wave on the ring A affects the phase of the chemical wave on ring B. Therefore, the phase difference between the chemical waves on the two rings is determined only by the shape of the reaction field. This difference in phase on the two circular rings is set as $\Delta\theta_0$. In the latter case, in contrast, the chemical wave on the ring A does not affect the chemical wave propagation on ring B. These two cases are selected by the initial phase difference between θ_L and θ_R when they reach a stationary propagation without collision. This characteristic phase difference $\Delta\theta_0$ is analytically derived in the Appendix.

When the initial phase difference is smaller than $|\Delta\theta_0|$, the phase difference is maintained. In this paper, we do not show the experimental data corresponding to this case. On the other hand, when the initial phase difference is larger than $|\Delta\theta_0|$, the chemical waves on the two rings affect each other: If $\Delta\theta_0 < 0$ (region I), the phase difference is fixed as $\Delta\theta_0$. If $\Delta\theta_0 > 0$ (region II), the phase difference changes alternatively. Thus, the location of the collision of the two waves changes alternatively. Figure 5 shows a phase map that depends on R (the ratio between the inner and outer radii, r_{out}/r_{in}) and D (the ratio between the overlap and the inner radius, d/r_{in}). The characteristics of the chemical wave propagation shown in 1 and 2 in Figure 3 in the experiments correspond to regions I and II, respectively. The properties of chemical wave propagation on two equivalent circular rings can be understood analytically within this framework.

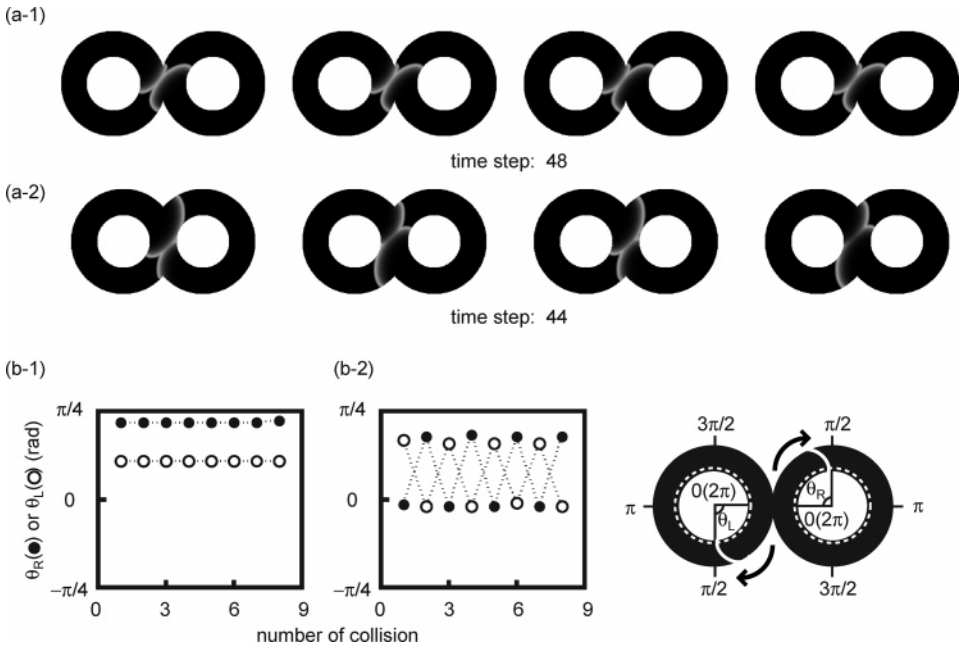

Figure 7. Results of a numerical simulation for a reaction field in the shape of a figure "8" composed of two equivalent circular rings based on the modified Oregonator model shown in eqs 7 and 8. (a) Snapshots of a typical nature of wave propagation for (a-1) slightly connected rings and (a-2) completely overlapping rings. (b) Spatio-temporal patterns of chemical wave propagation for (b-1) slightly connecting rings and (b-2) completely overlapping rings. The parameters and the initial conditions are the same as those in Figure 6. The shape of the field is $r_{out}/r_{in} = 2$ for both (1) and (2), $d/r_{in} = 2/9$ for (1), and $d/r_{in} = 1$ for (2).

c. Numerical Calculation Using the Modified Oregonator Model. We performed numerical calculations based on the modified Oregonator:[11,13]

$$\frac{\partial u}{\partial t} = \frac{1}{\epsilon}\left\{u(1-u) - (fv + A)\frac{u-q}{u+q}\right\} + D_u\nabla^2 u \qquad (7)$$

$$\frac{\partial v}{\partial t} = u - v + D_v\nabla^2 v \qquad (8)$$

where u and v are the dimensionless variable that correspond to the concentrations of the activator ($HBrO_2$) and the oxidized catalyst ($[Ru(bpy)_3]^{3+}$), respectively. f, ϵ, and q are the positive parameters that determine the nature of the BZ reaction, D_u and D_v are the diffusion constants for the activator and the oxidized catalyst, and A is the varible that is proportional to the light intensity. We set $A = 0.03$ in the brighter area and 0.005 in the darker area. The parameters used in the calculations are $f = 1.0$, $\epsilon = 0.05$, $q = 0.00015$, and $D_u = D_v = 1.0$. The chemical wave is initiated by setting $u = 0.5$ at a certain point. Some time later, the two chemical waves propagate in opposite directions. By increasing the variable for light intensity, A, in a certain area for some length of time, we can make one wave disappear, and a one-direction chemical wave is achieved.

The results of the numerical calculation for a reaction field in the shape of a circular ring are shown in Figure 6. The relationship between $\Delta\theta$ and r_{out}/r_{in} is described together with the analytical prediction by eq 6. This dependency is well described by the analytical discussion, and the experimental, theoretical, and numerical results are all consistent with each other.

Figure 7 shows the numerical results for a reaction field in the shape of a figure "8", which is composed of two equivalent circular rings. When the two circular rings slightly in contact one another, the phase difference is fixed at a constant value, as shown in Figures 7a-1 and b-1. On the other hand, when they completely overlap, the phase difference changes alternatively; i.e., the location of the collision changes alternatively, as shown in Figures 7a-2 and b-2. These experimental and analytical results are well reproduced by the numerical calculations.

Conclusion

The nature of wave propagation in the photosensitive BZ reaction on an excitable field in the shape of a circular ring and a figure "8" illuminated with a liquid-crystal projector were demonstrated. The chemical wave on a reaction field in the shape of a circular ring was observed and it is clarified that the shape of the chemical wave can be described as the involute of a circle. The velocity of the chemical wave depending on the inner and outer radii of the circular route was modulated at the intersection of the figure "8", and the location of collision then moved away from the intersection depending on the width of the ring. The spatio-temporal nature of wave propagation was observed by changing the degree of the intersection and the size of the route, even under different initial phase conditions for the two waves. These characteristics of chemical wave propagation were well reproduced by a numerical simulation based on the Oregonator model for the photosensitive BZ reaction.

Appendix

We consider chemical wave propagation on a field composed of two circular rings with overlap d, as shown in Figure 5. Here,

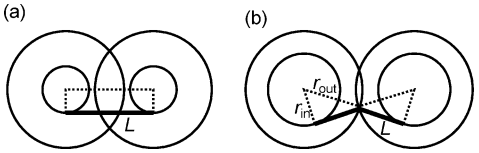

Figure 8. Schematic representation of the shortest path when the chemical wave in one ring propagates to the other ring: (a) when the shortest path is a straight line; (b) when the shortest path is a V-shaped line.

we derive the characteristic phase difference $\Delta\theta_0$ between the phase of the chemical wave in one ring (ring A) and that of the chemical wave on the other ring (ring B) after the chemical wave on the ring A affects chemical wave propagation on ring B. The time required for a chemical wave to reach a certain point can be calculated from the shortest path. Therefore, we have to consider the two cases as shown in Figure 8.

In the case in Figure 8a, i.e.,

$$\sqrt{{r_{out}}^2 - (r_{out} - d/2)^2} > r_{in} \qquad (9)$$

the shortest path from one ring to the other ring is a straight line, and the length, L, is

$$L = 2r_{out} - d \qquad (10)$$

If we suppose that the chemical on the ring A affects the chemical wave propagation on ring B, the phases of the chemical waves on rings A and B, θ_A and θ_B, can be written as

$$\theta_A = -\frac{\pi}{2} + \frac{v}{r_{in}}t$$

and

$$\theta_B = \frac{\pi}{2} + \frac{v}{r_{in}}\left(t - \frac{L}{v}\right)$$

where t is time. Therefore, the characteristic phase difference $\Delta\theta_0$ is derived as

$$\Delta\theta_0 = \theta_B - \theta_A = \pi - \frac{2r_{out} - d}{r_{in}} \qquad (11)$$

On the other hand, in the case of Figure 8b, i.e.,

$$\sqrt{{r_{out}}^2 - (r_{out} - d/2)^2} < r_{in} \qquad (12)$$

the shortest path is a V-shaped line, and L is derived as

$$L = 2\sqrt{{r_{out}}^2 - {r_{in}}^2} \qquad (13)$$

If we suppose that the chemical wave on ring A affects the chemical wave propagation on ring B, θ_A and θ_B can be written as

$$\theta_A = -\Theta_0 + \frac{v}{r_{in}}t \qquad (14)$$

and

$$\theta_B = \Theta_0 + \frac{v}{r_{in}}\left(t - \frac{L}{v}\right) \qquad (15)$$

where

$$\Theta_0 = \arccos\left(\frac{r_{in}}{r_{out}}\right) + \arccos\left(\frac{r_{out} - d/2}{r_{out}}\right) \quad (16)$$

Therefore, the characteristic phase difference $\Delta\theta_0$ is derived as

$$\Delta\theta_0 = \theta_B - \theta_A = 2\Theta_0 - \frac{2\sqrt{{r_{out}}^2 - {r_{in}}^2}}{r_{in}} \quad (17)$$

In summary, the characteristic phase difference $\Delta\theta_0$ is written as

$$\Delta\theta_0 = \theta_B - \theta_A = \begin{cases} \pi - 2R + D & (R > D/4 + 1/D) \\ 2\Theta_0 - 2\sqrt{R^2 - 1} & (R < D/4 + 1/D) \end{cases} \quad (18)$$

and

$$\Theta_0 = \arccos\left(\frac{1}{R}\right) + \arccos\left(R - \frac{D}{2}\right) \quad (19)$$

These equations are written in nondimensional form using $R = r_{out}/r_{in}$ and $D = d/r_{in}$. The phase map shown in Figure 5 is drawn according to the sign of $\Delta\theta_0$.

Acknowledgment. We thank Professor Masaharu Nagayama (Kanazawa University, Japan) for his helpful discussions regarding the mechanism. This study was supported in part by a Grant-in-Aid for Scientific Research from the Ministry of Education, Culture, Sports, Science, and Technology of Japan (No. 16550124) to S. N.

References and Notes

(1) Winfree, A. T. *The Geometry of Biological Time*; Springer: Berlin, 1980.
(2) Hall, Z. W. Ed. *Molecular Neurobiology*; Sinauer Pub.: Sunderland, MA, 1992.
(3) Murray, J. D. *Mathematical Biology*; Springer: Berlin, 1989.
(4) Kuhnert, L. *Nature* **1986**, *319*, 393.
(5) Kuhnert, L.; Agladze, K. I.; Krinsky, V. I. *Nature* **1989**, *337*, 244.
(6) Rambidi, N. G.; Shamayaev, K. E.; Peshkov, G. Y. *Phys. Lett. A* **2002**, *298*, 375.
(7) Sakurai, T.; Mihaliuk, E.; Chirila, F.; Showalter, K. *Science* **2002**, *296*, 2009.
(8) Tóth, A.; Showalter, K. *J. Chem. Phys.* **1995**, *103*, 2058.
(9) Steinbock, O.; Kettunen, P.; Showalter, K. *J. Phys. Chem.* **1996**, *100*, 18970.
(10) Motoike, I.; Yoshikawa, K. *Phys. Rev. E* **1999**, *59*, 5354.
(11) Ichino, T.; Igarashi, Y.; Motoike, N. I.; Yoshikawa, K. *J. Chem. Phys.* **2003**, *118*, 8185.
(12) Gorecka, J.; Gorecki, J. *Phys. Rev. E* **2003**, *67*, 067203.
(13) Nagahara, H.; Ichino, T.; Yoshikawa, K. *Phys. Rev. E* **2004**, *70*, 036221.
(14) Zaikin, A. N.; Zhabotinsky, A. M. *Nature* **1970**, *225*, 535.
(15) Field, R. J., Burger, M., Eds. *Oscillations and Traveling Waves in Chemical Systems*; Wiley: New York, 1985.
(16) Kapral, R., Showalter, K., Eds. *Chemical Waves and Patterns*; Kluwer Academic: Dordrecht, The Netherlands, 1995.
(17) Lázár, A.; Noszticzius, Z.; Försterling, H.-D.; Nagy-Ungvárai, Z. *Physica D* **1995**, *84*, 112.
(18) Steinbock, O.; Kettunen, P.; Showalter, K. *Science* **1995**, *269*, 1857.
(19) Winston, D.; Arora, M.; Maselko, J.; Gáspár, V.; Showalter, K. *Nature* **1991**, *351*, 132.
(20) Iguchi, Y.; Takitani, R.; Miura, Y.; Nakata, S. *Rec. Res. Devel. Pure Appl. Chem.* **1998**, *2*, 113.
(21) Motoike, N. I.; Yoshikawa, K.; Iguchi, Y.; Nakata, S. *Phys. Rev. E* **2001**, *63*, 036220.
(22) Yoshida, R.; Takahashi, T.; Yamaguchi, T.; Ichijo, H. *J. Am. Chem. Soc.* **1996**, *118*, 5134.
(23) Aliev, R. R.; Agladze, K. I. *Physica D* **1991**, *50*, 65.
(24) Agladze, K.; Aliev, R. R.; Yamaguchi, T.; Yoshikawa, K. *J. Phys. Chem.* **1996**, *100*, 13895.
(25) Kádár, S.; Amemiya, T.; Showalter, K. *J. Phys. Chem. A* **1997**, *101*, 8200.
(26) Gorecki, J.; Yoshikawa, K.; Igarashi, Y. *J. Phys. Chem. A* **2003**, *107*, 1664.
(27) Amemiya, T.; Yamamoto, T.; Ohmori, T.; Yamaguchi, T. *J. Phys. Chem. A* **2002**, *106*, 612.
(28) Müller, S. C.; Plesser, T.; Hess, B. *Physica D* **1987**, *24*, 87.
(29) Volford, A.; Simon, P. L.; Farkas, H.; Noszticzius, Z. *Physica A* **1999**, *274*, 30.
(30) Lázár, A.; Noszticzius, Z.; Farkas, H.; Försterling, H. D. *Chaos* **1995**, *5*, 443.
(31) Lázár, A.; Försterling, H.-D.; H. Farkas, Simon, P.; Volford, A.; Noszticzius, Z. *Chaos* **1997**, *7*, 731.